ResearchGate

See discussions, stats, and author profiles for this publication at: https://www.researchgate.net/publication/262178094

A Supramolecular Assembly Formed by Heteroassociation of Ciprofloxacin and Norfloxacin in the Solid State: Co-Crystal Synthesis and Characterization

ARTICLE *in* CRYSTAL GROWTH & DESIGN · MARCH 2013

Impact Factor: 4.89 · DOI: 10.1021/cg301299e

CITATIONS
4

READS
22

4 AUTHORS, INCLUDING:

Norma R Sperandeo
National University of Cordoba, Argentina
28 PUBLICATIONS **190** CITATIONS

SEE PROFILE

Available from: Norma R Sperandeo
Retrieved on: 31 January 2016

CRYSTAL GROWTH & DESIGN

Article

pubs.acs.org/crystal

A Supramolecular Assembly Formed by Heteroassociation of Ciprofloxacin and Norfloxacin in the Solid State: Co-Crystal Synthesis and Characterization

Graciela Pinto Vitorino,[†] Norma R. Sperandeo,[‡] Mino R. Caira,*[,§] and María R. Mazzieri*[,‡]

[†]Departamento de Farmacia, FCN, Universidad Nacional de la Patagonia SJB, Km. 4, 9000, Comodoro Rivadavia, Chubut, Argentina

[‡]Departamento de Farmacia, FCQ, Universidad Nacional de Córdoba, Pabellón Ciencias 2, Ciudad Universitaria, 5000, Córdoba, Argentina

[§]Department of Chemistry, University of Cape Town, Rondebosch 7701, South Africa

Supporting Information

ABSTRACT: The interaction in the solid state between ciprofloxacin (CIP) and norfloxacin (NOR) was investigated and a new multicomponent molecular complex (COP) was obtained and characterized. It is composed of equimolar quantities of both compounds, according to TLC and ^{1}H NMR data. As single-crystal X-ray analysis showed, COP crystallizes in the triclinic system, space group $P(\bar{1})$. The asymmetric unit comprises three independent zwitterions (A, B, and C) with contributions of both CIP and NOR, as well as 14.6 water molecules. At the zwitterion A site, the occurrence is about 37% (CIP), 63% (NOR); at the B site, there is predominantly CIP (70%); and at the C site the occurrence is about 43% (CIP) and 57% (NOR), yielding an overall 1:1 CIP-NOR ratio in the crystal. TG data evidenced a one-step loss of solvent (about 18% per COP zwitterion) below 110 °C, confirming the presence of water molecules. The propensity for heteroassociation between CIP and NOR, under the conditions described herein, originated a co-crystal reported for the first time between FQs, and became one of the most interesting aspects of this research.

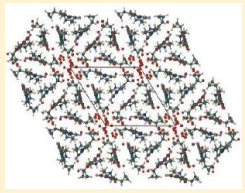

1. INTRODUCTION

Norfloxacin, 1-ethyl-6-fluoro-1,4-dihydro-4-oxo-7-(1-piperazinyl)-3-quinolinecarboxylic acid (NOR), and ciprofloxacin, 1-cyclopropyl-6-fluoro-4-oxo-7-(piperazin-1-yl)-1,4-dihydroquinoline-3-carboxylic acid (CIP) (Figure 1), are synthetic broad-spectrum antibacterial compounds belonging to the group of fluoroquinolone (FQ) antibiotics.[1,2] The accepted molecular mechanism of action of FQs would include their interaction with the enzyme-bound DNA complex that results in the inhibition of normal DNA gyrase or topoisomerase activity. To date, at least four structural models have been described for that interaction.[3−6] One of them was proposed by Shen et al. based on the packing of nalidixic acid molecules in crystals, among other experimental results.[3] A cooperative phenomenon that includes the self-association of FQs while they interact with DNA strands and enzyme was suggested. In this case, two types of interactions between FQs are feasible: $\pi-\pi$ stacking involving the aromatic rings and tail-to-tail hydrophobic interactions between the N-1 substituent groups. Also, intermolecular electrostatic attraction could bind ionized FQ molecules, through carboxylate and ammonium groups.[3] The self-association between NOR molecules in solution[7] and in the solid state has been reported,[8,9] whereas the same type of interaction between CIP molecules was only described in the solid state.[10]

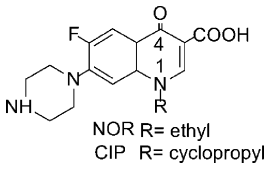

Figure 1. Molecular structure of ciprofloxacin (CIP) and norfloxacin (NOR) and atomic numbering used in this study.

On the other hand and with the aim of improving the NOR solubility, various co-crystals and salts have been prepared. For example, NOR forms co-crystals with isonicotinamide,[11] saccharin,[12] flavonoids, monoterpenes, amino acids, alkaloids, vitamins and nutraceuticals;[13] and salts with hydrochloric acid,[14] nicotinic acid,[15] oxalic acid, benzoic acid, tartaric acid, citric acid, malic acid,[16] succinic acid,[11,16] malonic acid,[11] maleic acid,[11] and saccharin.[17] The heteroassociation of CIP with various salts such as anhydrous CIP hydrochloride,[18] CIP hydrochloride monohydrate,[19] CIP hydrochloride 1.34-hydrate,[20] CIP lactate sesquihydrate,[10] CIP saccharinate,[17] CIP hemi sodium salt pentahydrate, and CIP sodium salt pentahydrate was described as well.[21] Furthermore, co-crystals of CIP with phenolic compounds, flavonoids, monoterpenes, amino acids, alkaloids, vitamins, and nutraceuticals have been prepared and characterized.[13]

As part of our ongoing interdisciplinary medicinal chemistry project, aimed at improving the biological and pharmaceutical properties of antibacterial FQs in clinical use, we proposed to

Received: September 6, 2012
Revised: January 15, 2013
Published: February 1, 2013

ACS Publications © 2013 American Chemical Society

study the association of different FQ molecules, in solution and in the solid state. This approach could overcome some pharmacokinetic and toxicological problems of these important antibiotics[1,2] as combinations of sulfa drugs have done.[22,23] The results reported herein have focused on the research of NOR and CIP association in the solid state, originating a co-crystal. It should be noted that although CIP and NOR have been thoroughly characterized in the solid state, both individually and co-crystallized with different compounds,[8,24−28] as far as we know, the heteroassociation between themselves has not been studied yet. Therefore, in this contribution we present the preparation and physical characterization of a new 1:1 CIP:NOR supramolecular assembly (COP) obtained by coprecipitation from vapor diffusion of AcOH into an aqueous alkaline solution of CIP and NOR. To identify and assess the chemical composition of the sample we used ^{1}H nuclear magnetic resonance spectroscopy (^{1}H NMR). Differential scanning calorimetry (DSC), thermogravimetry (TG), polarized light microscopy (PLM), hot stage microscopy (HSM), powder X-ray diffraction (PXRD) and single-crystal X-ray diffraction (SXRD) have been applied to characterize this new co-crystal.

2. EXPERIMENTAL SECTION

2.1. Materials and COP Preparation. CIP and NOR were kindly supplied by Roux Ocefa (Argentina) and Parafarm (Argentina), respectively. Their purity was confirmed by melting point (mp) determination and thin layer chromatography (TLC). AcOH (Cicarelli) and NaOH (Anedra), DMSO-d_6 (Merck), chloroform (Cicarelli), methanol (Dorwill), toluene (Biopack), dichloromethane (Cicarelli), aqueous ammonia (Cicarelli), silicone oil (Sigma), and sodium edetate (Anedra) were obtained from commercial suppliers and were used without further purification.

For the preparation of COP, 100.0 mg of CIP (0.30 mmol) and 96.4 mg of NOR (0.30 mmol) were dissolved in 10 mL of aqueous 0.3 M NaOH. The resulting solution was then transferred to a small beaker, which was introduced into a screw tapped vessel containing 50 mL of aqueous 0.3 M AcOH. The vessel was tightly closed and stored in the dark at room temperature (20−25 °C) until a precipitate was formed (approximately two months). The mother liquor had a final pH = 4.2. The precipitate was collected by vacuum filtration, washed with cold distilled water, and dried in a desiccator over solid NaOH, at room temperature and under a mild vacuum provided by a water aspirator pump.

CIP and NOR were precipitated by the same procedure described for COP. Each precipitate was collected by vacuum filtration, washed with cold distilled water, and dried in a vacuum desiccator over NaOH and then at 100 °C, 0.35 mmHg, over P_2O_5 until a constant weight was obtained.

Another sample of COP was dried with the procedure described for CIP and NOR.

2.2. Thin Layer Chromatography. TLC analyses were carried out on silica gel 60 F_{254} plates previously treated with 0.27 mol/L sodium edetate solution adjusted to pH 7.0. The mobile phase had the composition chloroform/methanol/toluene/dichloromethane/aqueous ammonia (2.7:4.6:1.7:0.5:0.5, v/v).[29] The spots were visualized with ultraviolet light.

2.3. Melting Point. All mp determinations were carried out by the capillary tube method and are reported without correction.

2.4. ^{1}H Nuclear Magnetic Resonance Spectroscopy. The ^{1}H NMR characteristics of COP, CIP, and NOR in DMSO-d_6 solutions (5 mg/mL) were studied at 25 °C by using a Bruker Avance II 400 spectrometer (current probe 5 mm BBI 1H/D-BB Z-GRD Z8202/0349). The spectra were obtained with a spectral width of 20 ppm using a 30° pulse (7.09 μs) and 16 scans. The center of the solvent peak was used as an internal standard. The processing of the data was performed with a Bruker Standard program (TOPSPIN 2.0).

2.5. Single-Crystal X-ray Diffraction. Intensity data for SXRD analysis were collected on a Bruker Kappa DUO APEX II diffractometer and processed using APEX2 and SAINT software.[30] The crystal specimen was mounted on a cryogenic loop using Paratone N oil (Exxon, USA) and cooled to 173(2) K in a constant stream of nitrogen vapor produced at a flow rate of 20 mL/min by a Cryostream cooler (Oxford Cryosystems, UK). The basic structure was revealed using SHELXS-97.[31] However, development and refinement of the model was not a routine procedure owing to the subtle nature of the COP phase, being a "mixed" crystal in which three unique molecular sites (A, B, C) in the crystal asymmetric unit are each occupied by very closely related zwitterions, in this case CIP and NOR, to different extents. Modeling of the structure thus required very extensive analysis of successive difference Fourier maps and careful treatment of site-occupancies and thermal parameters, as well as positional disorder of included water molecules. Further details are given in the discussion. Full-matrix least-squares refinement on F^2 proceeded with SHELXL-97[31] operating under the program interface X-Seed.[32] Non-hydrogen atoms of the drug molecules refined anisotropically. Water oxygen atoms (14.6 in the asymmetric unit) were distributed over 28 sites. Only seven sites were fully occupied and these oxygen atoms refined anisotropically while the remaining disordered atoms were treated isotropically with a common thermal parameter set at the average of those of the ordered water O atoms. Treatment and implications of the drug disorder are described in some detail in Section 3 below. The zwitterionic nature of the drug molecules was evident from unequivocal location of their H atoms. The latter were generally added in a riding model with U_{iso} values 1.2−1.5 times those of their parent atoms. Due to the significant disorder, H atoms of water molecules were not included in the model.

2.6. Differential Scanning Calorimetry and Thermogravimetry. The DSC and TG measurements were recorded on MDSC 2920 and TG 2950 analyzers (TA Instruments Inc., USA), respectively, at a heating rate of 10 °C/min under N_2 (99.99% purity, flow rate of 50 mL/min). For DSC measurements, crimped aluminum pans were used. The DSC and TG temperature axes were calibrated with indium (99.99% purity, mp 156.6 °C) and the Curie point of Ni (358.1 °C), respectively. Empty aluminum pans were used as references. Samples with mass 1−2 mg were employed. Data were treated with Universal Analysis 2000 software (TA Instruments Inc.).

2.7. Kofler Hot-Stage Microscopy. The physical and morphological changes of the samples that occurred during the process of heating were observed through a microscope fitted with a Kofler hot-stage (Leitz, Wetzlar, Germany) with a magnification of 10×. Each sample was immersed in high-boiling silicone oil to detect any bubble evolution (dehydration or decomposition events) and heated at an initial rate of 10 °C/min and at 1 °C/min on approaching the mp.

2.8. X-ray Powder Diffraction. PXRD patterns were collected using a Philips PW 1710-BASED diffractometer. The operating conditions were as follows: 40 kV, 20 mA with Cu Kα_1 radiation (λ = 1.54056 Å) source, 3.0−46° 2θ (step size of 0.04° 2θ) and a scan rate of 1.000 s/step. Data were treated with the PC-APD software.

3. RESULTS AND DISCUSSION

3.1. Preliminary Characterization of the COP Crystals. Colorless prisms of CIP (Figure 2a) and needle-like crystals of NOR (Figure 2b) were isolated through the precipitation procedures described in the Experimental Section. Crystals of COP (Figure 2c) were colorless prisms, similar to CIP. The crystals were of variable sizes (up to 0.2 mm long).

According to TLC results, COP was composed of CIP and NOR since two spots were detected, which matched those of CIP (R_f = 0.43) and NOR (R_f = 0.30) used as references. Furthermore, co-crystals of COP consist of CIP and NOR in a 1:1 molar ratio according to ^{1}H NMR evidence. Indeed, the spectrum (Figure 3) showed all the signals corresponding to both APIs,[33] and the areas under the signals at 8.67 and 8.94

dx.doi.org/10.1021/cg301299e | Cryst. Growth Des. 2013, 13, 1050−1058

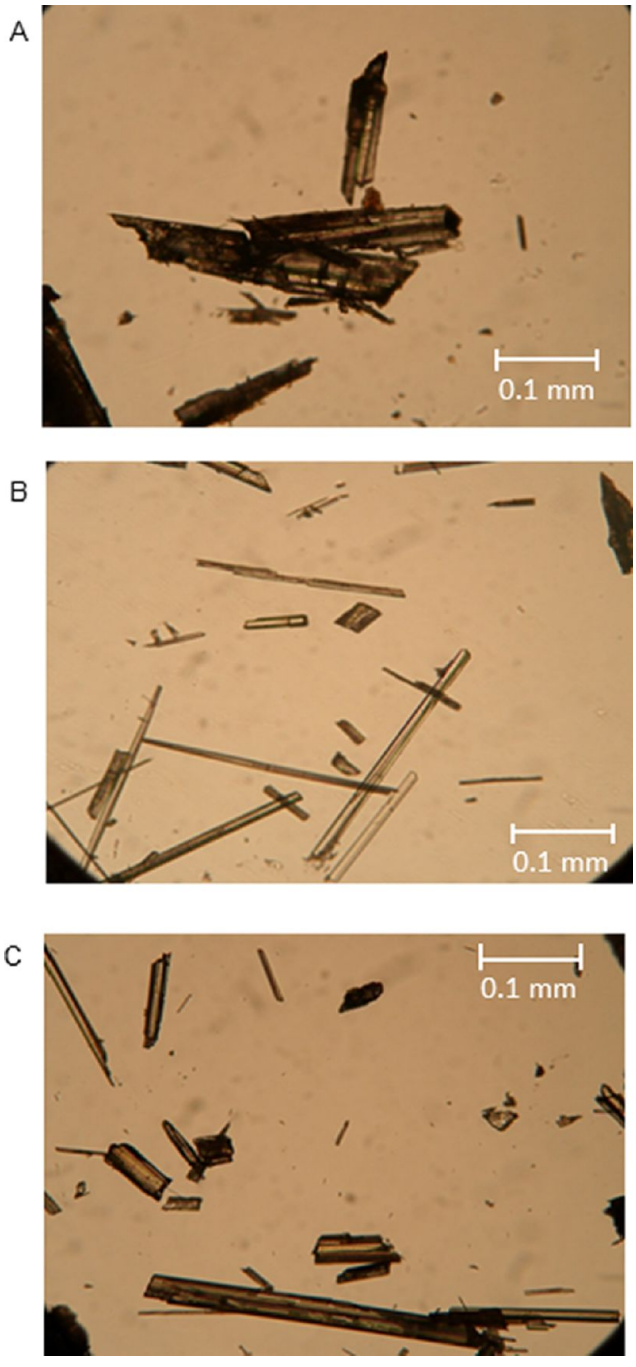

Figure 2. Optical images (10×) of the crystals of (A) CIP, (B) NOR, and (C) COP.

ppm, assigned to the H-2 of CIP and NOR respectively, were comparable.

Table 1 presents the mp data for CIP, NOR, and COP, and includes for comparison the corresponding data reported in the literature for each of the FQs. As can be seen, the mp of CIP and NOR agree well with the reported ones,[25,26,34,35] whereas the mp of COP was different to those of the APIs, suggesting the formation of a new solid phase.

3.2. Single Crystal X-ray Diffraction. When the X-ray analysis of COP was undertaken in our laboratory, a survey of previous crystallographic studies indicated that a considerable number of phases of CIP and NOR were already reported. The crystal properties of several solid phases of NOR were extensively explored yielding two anhydrous forms,[8,9,36] several hydrates (1.125 hydrate, 1.25 hydrate,[37] sesquihydrate,[9,25,38,39] dihydrate,[40] hemipentahydrate, trihydrate, and pentahydrate[41]) and an amorphous form.[36,42] On the other hand, the known crystal forms of CIP free base at that time were anhydrates,[14,21,43,44] as well as hydrate[44] and hexahydrate phases.[27]

The crystallographic data and refinement parameters for the X-ray analysis of COP are presented in Table 2. The average formula quoted for the COP phase from the crystal structure analysis is consistent with the NMR data that indicated a 1:1 molar ratio of CIP and NOR in the solid state. Water contributions from the results of the least-squares refinement yielded a complete formula for the COP phase. From the average formula, the water content is equivalent to ∼21% by mass, which is somewhat higher than that indicated by TG (17.9 ± 0.8%, details below). However, the discrepancy can be attributed to both the difficulty of accurate refinement of site-occupancy factors (s.o.f.s) of water O atoms (extent of disorder 52%) as well as the fact that the crystal used for data-collection suffered no exposure to the atmosphere during manipulations for crystal preparation and data capture, having been immediately protected in oil, whereas more significant water loss might have occurred during TG manipulations.

The crystal asymmetric unit (Figure 4) contains three independent zwitterions (labeled A, B, C), each of which was found to be a superposition of CIP and NOR molecules in different ratios, initially established from difference electron-density maps, and subsequently confirmed by the crystallographic refinement.

The molecular entities A, B, and C are all zwitterions characterized by the presence of a carboxylate moiety, while the terminal nitrogen atom of the piperazinyl ring is protonated (Figure 5). This state of each molecule was established unequivocally by evaluation of carboxylate C−O distances (range 1.244(4)−1.278(4) Å, $n = 6$), the absence of a hydrogen atom on the −COO moiety, and the actual location of a hydrogen atom on the piperazinyl N atom. In the early stages of the analysis, a careful study of difference Fourier syntheses revealed that the two atoms C23 and C24 (Figure 5), which would be chemically equivalent atoms if CIP alone were present at each of the three molecular sites, actually displayed unequal electron-densities in all three of the zwitterions A, B, and C. This finding was consistent with the notion of a mixed 1:1 CIP-NOR phase deduced by NMR analysis and the X-ray model could thus be developed by taking into account the observed CIP-NOR molecular overlap at each of the three sites. Specifically, the procedure employed was to place all atoms on each molecule (except C23 and C24) and refine them, and use the subsequent difference electron-densities at the C23 and C24 sites as initial measures of the relative site-occupancy factors (s.o.f.s) of these two atoms. In Figure 5, it is shown that atom C23 in each of the three zwitterions was initially assigned a full site-occupancy factor (s.o.f. = 1.0, corresponding to 100% presence of a C atom at that position), based on its relatively high electron-density. Instead, the atoms labeled C24 in each molecule had significantly lower electron-densities than those of their C23 counterparts, with some variation in the values for zwitterions A−C. Successive refinements involved alternating the least-squares optimization of the s.o.f.s of atoms C24 with varying thermal parameters, followed by release of the s.o.f.s and variation in the thermal parameters, eventually fixing the refined s.o.f.s at convergence. The final assignments also took

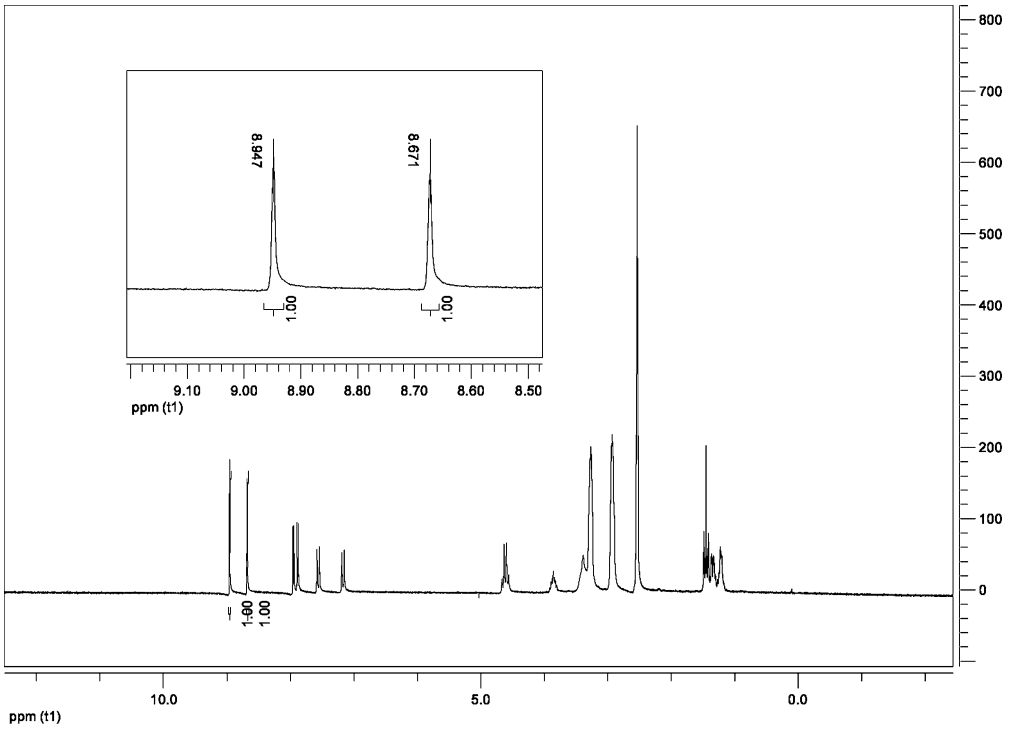

Figure 3. ^{1}H-NMR (DMSO-d_6) spectrum of COP. The inset indicated the peaks assigned to the H-2 of CIP (8.67 ppm) and NOR (8.94 ppm).

Table 1. Melting Points (mp) Determined by the Capillary Tube Method for CIP, NOR, and COP

sample	mp (°C)	reported mp (°C)
CIP	269–270[a]	255–257[34]
		270–275[35]
NOR	217–219[a]	220–222[34]
		217–219[35]
COP	229–230[a]	
	227–229[b]	

[a]Samples dried at 100 °C, 0.35 mmHg, and over P_2O_5, [b]Sample dried over NaOH, at room temperature, under a mild vacuum provided by a water aspirator pump.

Table 2. Crystal Data and Refinement Parameters for the COP Crystal

average formula	$C_{16.5}H_{18}N_3O_3F{\cdot}4.86H_2O$
formula mass (g mol^{-1})	412.88
crystal system	triclinic
space group	$P(\bar{1})$
a (Å)	13.873(2)
b (Å)	15.906(3)
c (Å)	16.329(3)
α (°)	116.103(3)
β (°)	103.817(3)
γ (°)	102.245(3)
V (Å^3)	2926.7(8)
Z	6
D_c (g cm^{-3})	1.406
crystal size (mm)	0.03 × 0.07 × 0.18
T (K)	173(2)
λ (MoKα) (Å)	0.71073
θ-range (°)	2.19–29.24
h k l limits	−19: 17; −21: 20; −14: 22
absorption correction	empirical (SADABS)
reflections (total/unique/R_{int})	28476/15670/0.0339
observed reflections [$I_o > 2\sigma(I_o)$]	9046
completeness (%)	98.5
restraints/parameters	0/796
R_1 (observed data/all data)	0.0768/0.1327
wR_2 (observed data/all data)	0.2038/0.2392
S (goodness-of-fit on F^2)	1.042
$\Delta\rho_{max,\ min}$ (e Å^{-3})	0.808, −0.509
CCDC deposition no.	887955

into account to some extent geometric parameters [in particular (aromatic) N−C−C23 and (aromatic) N−C−C24 angles, which tend to be different for CIP and NOR species found in the Cambridge Database.[45] Figure 5 shows the values of the final s.o.f.s of atoms C23 and C24. For the three independent molecular sites, this particular partitioning would be interpreted as follows, all three containing contributions to both CIP and to NOR: at the A site, CIP occurs about 37% of the time and NOR about 63%; in contrast, at the B site there is predominantly CIP presence (70%) and 30% NOR contribution and finally, at the C site, CIP and NOR are present in roughly equal proportions (43% and 57% respectively). The resulting total atom count thus yields the average formula for the COP phase quoted in Table 2.

It should be noted that in crystallographic refinement with this unusual type of molecular disorder, various combinations of s.o.f. and thermal parameters that describe the vibration of the respective disordered atoms are possible and could be equally "acceptable". However, in this case the values indicated in Figure 5 were based on initial experimental values of difference electron-density that were subsequently optimized, ensuring that the overall 1:1 CIP-NOR composition was eventually met. A minor point is that in modeling CIP and NOR molecules at the same site, only the H atoms for the CIP contribution were included in the calculation because of the intractability of adding H atoms (methylene and methyl)

dx.doi.org/10.1021/cg301299e | Cryst. Growth Des. 2013, 13, 1050−1058

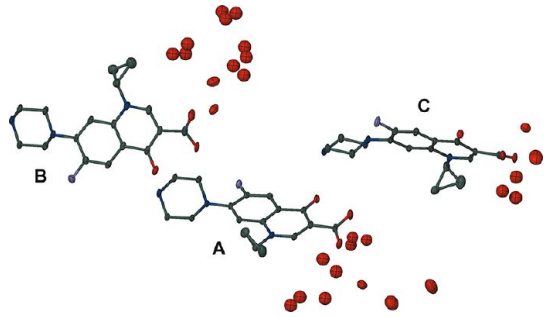

Figure 4. The crystallographic asymmetric unit of COP with anisotropically refined atoms shown as thermal ellipsoids drawn at the 50% probability level and isotropic atoms shown as spheres. H atoms are omitted for clarity. Oxygen atoms (including those of water molecules) are shown in red.

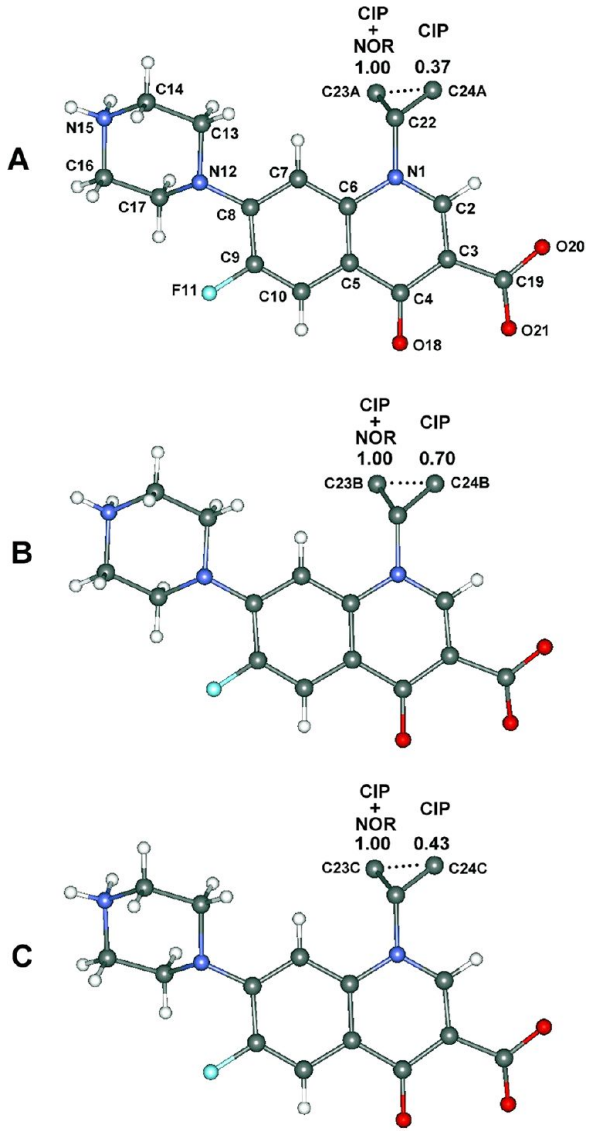

Figure 5. Refined site-occupancy factors of atoms C23 and C24 of each of the three crystallographically independent zwitterions in the crystal of COP. (The common atomic numbering scheme is indicated for zwitterion A.)

simultaneously to cater for the NOR contributions. Methylene H atom contributions on atoms C24 do, however, have the same s.o.f.s as their parent atoms.

Subsequent to the X-ray analysis of the COP crystal, the authors were alerted to a recent report of the crystal structure of a new phase of CIP,[46] with formula $3(\text{CIP})\cdot 14.5\text{H}_2\text{O}$, unit cell parameters a = 13.876(1), b = 15.876(1), c = 16.258(2) Å, α = 115.755(7), β = 103.610(7), γ = 102.325(5)°, space group $P(\bar{1})$ and Z = 2 (i.e., three independent CIP zwitterions in the asymmetric unit). Comparison of these data with those listed for COP in Table 2 shows that the new CIP phase is the ordered, isostructural equivalent of the COP phase in which all three molecular sites are fully occupied by CIP zwitterions exclusively. We note also that the water content of the new phase is ~4.8 molecules per drug molecule, which is practically identical to what we modeled in the analysis of the COP phase. Since a full geometrical description of the isostructural arrangement in $3(\text{CIP})\cdot 14.5\text{H}_2\text{O}$ has been published,[46] only a very brief description of the molecular association in the crystal of COP is warranted here to avoid repetition.

The crystallographically independent CIP-NOR zwitterions A, B, and C form individual linear arrays *via* $\text{N}^+-\text{H}\cdots{}^-\text{O}-\text{C}$ hydrogen bonds (Figure 6), the donor H atom being that occupying the *equatorial* position on nitrogen atom N15. We note that for arrays A and B, the respective H-bond acceptor carboxylate oxygen atoms (O21) are spatially equivalent, whereas array C is unique in using the alternative carboxylate oxygen atom (O20) as acceptor. The lengths of the three unique charged-assisted hydrogen bonds are, however, indistinguishable. Full geometrical data for the principal hydrogen bonds appear in Table 3.

The arrays A, B, C in Figure 6 self-assemble in the form of a "triangular prism" that propagates parallel to the crystal *a*-axis (Figure 7), the prism being maintained by four unique intermolecular hydrogen bonding interactions $\text{N}^+-\text{H}\cdots{}^-\text{O}-\text{C}$ among the symmetry-independent zwitterions (A, B, C), in each instance involving the *axial* H atom on the respective nitrogen atoms as the donor. The A···B association and the A···C association each involve a single N^+-H···$^-$O−C hydrogen bond with keto oxygen atom O18 as acceptor, while the B···C association is effected *via* bifurcated hydrogen bonds of type $\text{N}^+-\text{H}\cdots\text{O}{=}\text{C}$ and $\text{N}^+-\text{H}\cdots{}^-\text{O}-\text{C}$, the respective acceptor atoms being the keto oxygen O18 and the carboxylate atom O21 (Table 3).

For the most part, the water molecules cluster within channels parallel to the crystal *a*-axis, these channels being located at the apexes of the triangular prisms formed by the CIP-NOR molecules. This is shown in Figure 8 (bottom), a projection of the crystal structure down the *a*-axis, which illustrates the pseudohexagonal arrangement of the drug molecules. There is also regular $\pi-\pi$ stacking between each fluorophenyl residue on a given face of the triangular prism and the corresponding residue on the inversion-related face. The relevant ring centroid-centroid distances are 3.513(2) Å (A···A), 3.528(2) Å (B···B), and 3.620(2) Å (C···C). Hydrogen bonding involving water molecules is very complex, given the high level of their disorder. They are extensively hydrogen bonded to one another and to the N−H units of the drug molecules.

3.3. DSC, TG, HSM, and PXRD. In order to investigate further the thermal behavior of COP and to confirm that COP was a solvated solid, the DSC and TG curves of COP and the DSC traces of CIP and NOR, crystallized under the same

dx.doi.org/10.1021/cg301299e | *Cryst. Growth Des.* 2013, 13, 1050−1058

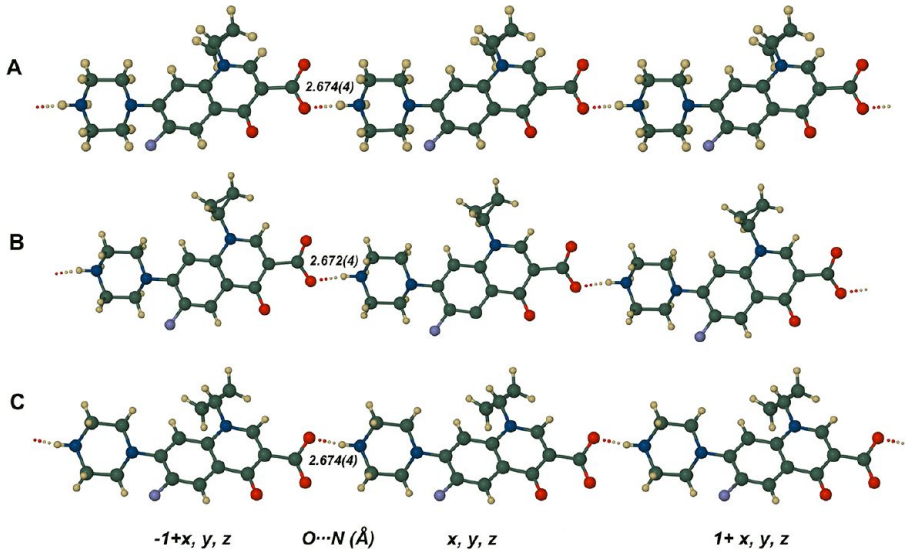

Figure 6. Linear hydrogen bonded arrays formed by the three independent zwitterions A, B, and C in the crystal of COP.

Table 3. Hydrogen Bond Data for COP[a]

D−H···A	d(D−H) (Å)	d(H···A) (Å)	d(D···A) (Å)	DHA, deg
N15A−H15A···O21A^{i}	0.92	1.76	2.674(4)	172
N15B−H15D···O21B^{i}	0.92	1.77	2.672(4)	168
N15C−H15E···O20C^{i}	0.92	1.76	2.674(4)	171
N15A−H15A···O18B	0.92	1.88	2.783(4)	167
N15B−H15C···O18C^{ii}	0.92	2.25	2.878(3)	125
N15B−H15C···O21C^{ii}	0.92	2.04	2.886(4)	152
N15C−H15F···O18A	0.92	2.06	2.838(3)	141

[a]Symmetry codes: (i): −1 + x, y, z; (ii): −2 + x, y, z.

experimental conditions as COP were obtained (Figure 9). It should be noted that both APIs were dried over P_2O_5 to obtain anhydrous samples and to compare their thermal behaviors with data reported in literature.[8,24−28] The crystals of COP were dried less vigorously (see experimental section 2.1) in order to maintain the full complement of water in the complex phase.

The DSC traces of CIP (Figure 9a) and NOR (Figure 9b) showed single melting endotherms at 270.1 °C (extrapolated onset, T_{onset}) and 216.7 °C (T_{onset}) respectively, followed by large exothermic peaks attributable to decomposition. The observed melting temperatures (T_{onset}) were in good agreement with the ones reported by Li et al.[44] for anhydrous CIP (270.8 °C) and by Sustar et al.[47] and Barbas et al.[8] for polymorph A of NOR (218.5−220 °C). On the other hand, the DSC trace of COP (Figure 9c), in addition to a broad melting endotherm at 228.9 °C (T_{onset}), exhibited a broad endothermic peak at 87.9 °C (T_{onset}) attributable to dehydration since it was accompanied by a one-step weight loss of 17.9 ± 0.8% in the respective TG trace (Figure 9d). This result confirmed that COP was a hydrated solid.

The thermal events just described for COP crystals were supported by the observations made by HSM. The colorless prisms of COP (immersed in silicone oil) showed abundant release of tiny bubbles between 95 and 110 °C, indicating the loss of solvent from the sample, which in turn was consistent with the DSC and TG results. At about 230 °C, the desolvated particles melted and upon further heating the molten phase

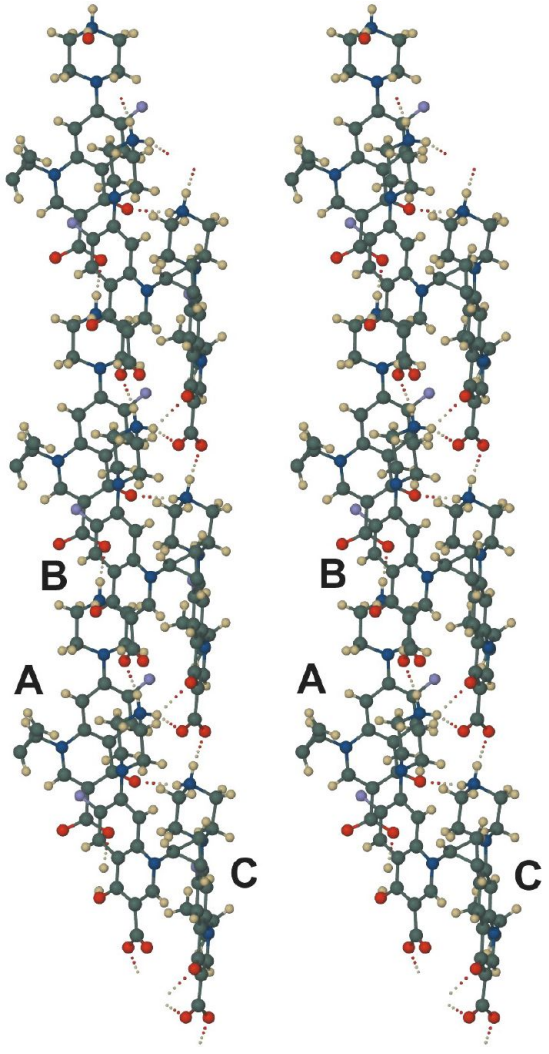

Figure 7. Stereoview illustrating the "triangular prism" formed by intermolecular hydrogen bonds (N^+−H···$^-$O−C) that link the linear arrays of zwitterions A, B, and C in the crystal of COP.

dx.doi.org/10.1021/cg301299e | Cryst. Growth Des. 2013, 13, 1050−1058

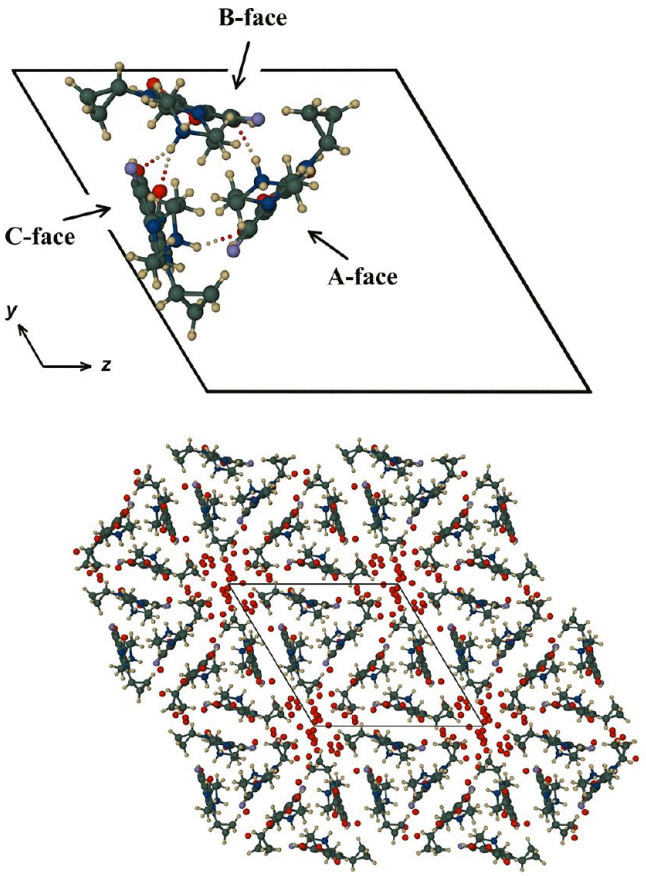

Figure 8. A portion of the infinite "triangular prism" assembly viewed down the *a*-axis (top). Crystal packing diagram projected down [100] (bottom). Isolated red circles represent water oxygen atoms.

diminished in size and turned up colored, typical of a decomposition process.

Thus, according to the DSC and HSM evidence, the DSC melting temperature of COP, as well as its mp (Table 1), were different to those of CIP and NOR and fell between them. This fact indicated that an interaction took place between CIP and NOR, which generated a solid sample with a thermal behavior different to those of its precursors, and this was in good accord with the SXRD data that revealed that COP was a new crystalline phase.

The PXRD patterns of CIP, NOR, and COP are shown in Figure 10. It should be noted that the diffractogram of CIP

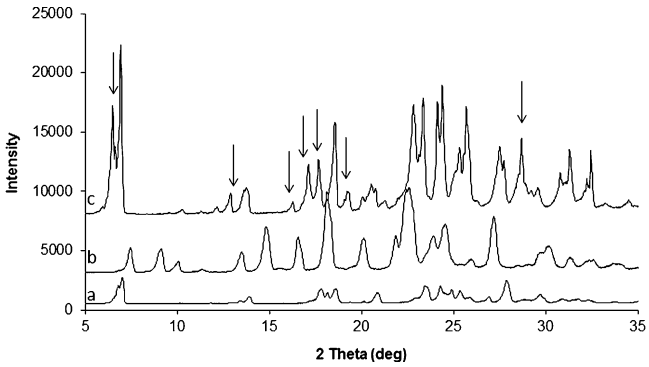

Figure 10. PXRD patterns of (a) CIP, (b) NOR, and (c) COP.

(Figure 10a) was similar to the one previously reported by Mahapatra et al.[43] for CIP anhydrate, and the PXRD pattern of NOR (Figure 10b) was in accordance with the one reported for NOR anhydrate.[38] The powder pattern of COP (Figure 10c) differed clearly from those of the individual APIs, indicating the presence of a new crystalline phase. In fact, several new reflections (marked with arrows in Figure 10c) were observed. Also, the absence of various characteristic reflections of CIP and NOR was noted, supporting the formation of a new crystalline phase, as indicated by SXRD.

4. CONCLUSIONS

It has been possible to obtain and characterize for the first time a new multicomponent molecular complex, COP, originating from the heteroassociation of CIP and NOR in the solid state. Both compounds are present in a 1:1 molecular relation, producing a mutually hydrated salt with an interesting supramolecular structure that is isostructural with a recently

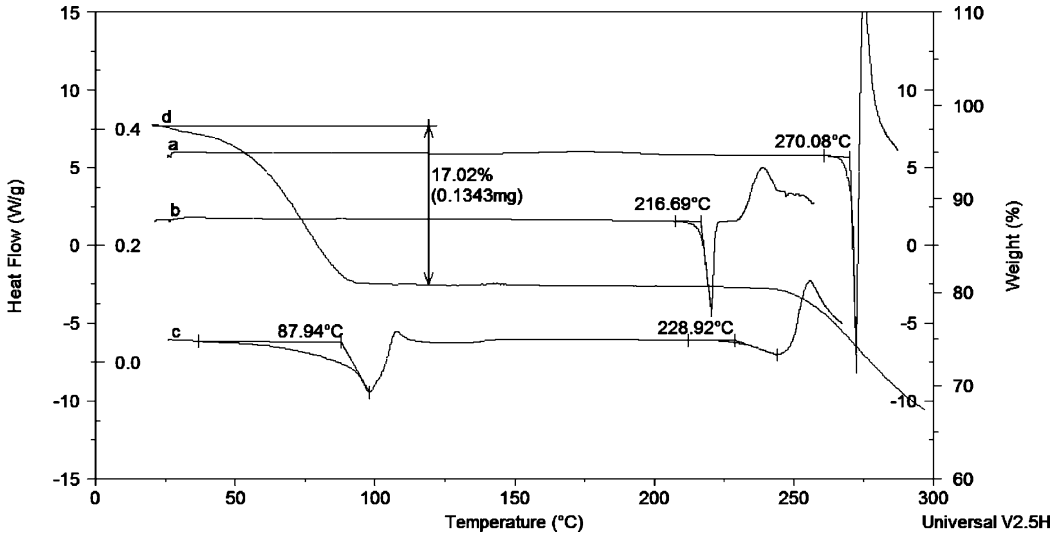

Figure 9. Overlaid DSC curves (crimped pan, 10 °C/min and flowing N_2 at 50 mL/min) of (a) CIP, (b) NOR, (c) COP, and (d) TG trace (10 °C/min and flowing N_2 at 50 mL/min) of COP. Samples of CIP and NOR were dried over P_2O_5, while COP was dried over NaOH.

dx.doi.org/10.1021/cg301299e | *Cryst. Growth Des.* 2013, 13, 1050−1058

discovered hydrated phase of CIP.[46] All the experimental data collected, such as melting temperatures, DSC profiles, and PXRD patterns, showed that COP has physical properties different from those of the pure components.

In the crystal, the molecules of CIP and NOR are ionized, assembling as "triangular prisms". Their interaction in the crystal occurs by stacking between adjacent molecules of CIP or NOR. In addition to N−H···O hydrogen bonding linking the molecules in linear chains, there is π-stacking between each fluorophenyl residue on a given face of the triangular prism and the corresponding residue on the inversion-related face. These kinds of interactions would be in accordance with those proposed by Shen et al.,[3] in the cooperative binding model, for the inhibition of DNA gyrase. Also, there is a complex and very extensive hydrogen bonding scheme in the resulting crystal structure, with water molecules being highly disordered.

The propensity for heteroassociation between CIP and NOR, under the conditions described herein, originated a co-crystal reported for the first time between FQs, and became one of the most interesting aspects of this research. The present results not only contribute to supporting the mechanism of action of FQs proposed by Shen et al., but also open new prospects for exploring synergistic antibacterial activity, decrease in adverse effects, improvement in pharmacokinetic and pharmaceutical properties of NOR and CIP, and the possibility of forming other co-crystals. All of these studies are in progress.

■ ASSOCIATED CONTENT

Supporting Information

CIF files giving crystal data for COP. This material is available free of charge via the Internet at http://pubs.acs.org

■ AUTHOR INFORMATION

Corresponding Author

*(M.R.M.) Tel. +54 351 5353850 (ext 53351). Fax. +54 351 5353850 (ext 53350). E-mail: mrmazzie@fcq.unc.edu.ar. (M.R.C.) Tel. +27 21 650 3071. Fax. +27 21 650 5195. E-mail: mino.caira@uct.ac.za.

Notes

The authors declare no competing financial interest.

■ ACKNOWLEDGMENTS

Financial support from SECyT-UNC and Agencia Nacional de Promoción Científica y Tecnológica of Argentina is gratefully acknowledged. The authors acknowledge F. Komrovsky for helping with DSC and TG measurements. M.R.C. thanks the University of Cape Town and the National Research Foundation (Pretoria) for research support.

■ REFERENCES

(1) Van Bambeke, F.; Michot, J. M.; Van Eldere, J.; Tulkens, P. M. *Clin. Microbiol. Infect.* **2005**, *11*, 256−280.

(2) Prabodh Chander, S.; Ankit, J.; Sander, J. *Acta Pol. Pharm. − Drug Res.* **2009**, *66*, 587−604.

(3) Shen, L. L.; Mitscher, L. A.; Sharma, P. N.; O'Donnell, T. J.; Chu, D. W. T.; Cooper, C. S.; Rosen, T.; Pernet, A. G. *Biochemistry* **1989**, *28*, 3886−3894.

(4) Palu, G.; Valisena, S.; Ciarrocchi, G.; Gatto, B.; Palumbo, M. *Proc. Natl. Acad. Sci. U. S. A.* **1992**, *89*, 9671−9675.

(5) Fan, J. Y.; Sun, D.; Yu, H.; Kerwin, S. M.; Hurley, L. H. *J. Med. Chem.* **1995**, *38*, 408−424.

(6) Heddle, J. G.; Maxwell, A. *Antimicrob. Agents Chemother.* **2002**, *46*, 1805−1815.

(7) Evstigneev, M. P.; Rybakova, K. A.; Davies, D. B. *Biophys. Chem.* **2006**, *121*, 84−95.

(8) Barbas, R.; Martí, F.; Prohens, R.; Puigjaner, C. *Cryst. Growth Des.* **2006**, *6*, 1463−1467.

(9) Puigjaner, C.; Barbas, R.; Portell, A.; Font-Bardia, M.; Alcobé, X. *Cryst. Growth Des.* **2010**, *10*, 2948−2953.

(10) Parsanna, M. D.; Guru Row, T. N. *J. Mol. Struct.* **2001**, *559*, 255−261.

(11) Basavoju, S.; Boström, D.; Velaga, S. P. *Cryst. Growth Des.* **2006**, *6*, 2699−2708.

(12) Velaga, S. P.; Basavoju, S.; Boström, D. *J. Mol. Struct.* **2008**, *889*, 150−153.

(13) Kruthiventi, A. K.; Roy, S.; Goud, R.; Javed, I.; Nangia, A.; Reddy, J. S. WO Patent 136408 A1, 2009.

(14) Turel, I.; Gruber, K.; Leban, I.; Bukovec, N. *J. Inorg. Biochem.* **1996**, *61*, 197−212.

(15) Simonovitch, H. U. S. Patent 4,792,552, 1988.

(16) Reedy, J. S.; Ganesh, S. V.; Nagalapalli, R.; Dandela, R.; Solomon, K. A.; Kumar, K. A.; Goud, N. R.; Nangia, A. *J. Pharm. Sci.* **2011**, *100*, 3160−76.

(17) Romañuk, C. B.; Manzo, R. H.; Garro Link, Y.; Chattah, A. K.; Monti, G. A.; Olivera, M. E. *J. Pharm. Sci.* **2009**, *98*, 3788−3801.

(18) Silva Sousa, F.; Oudenes, J.; Ivanovich Gorin, B. U. S. Patent 0300258 A1, 2008.

(19) Liu, Y.; Wang, J.; Yin, Q. *J. Cryst. Growth* **2005**, *276*, 237−242.

(20) Turel, I.; Golobic, A. *Anal. Sci.* **2003**, *19*, 329−330.

(21) Fabbiani, F. P. A.; Dittrich, B.; Florence, A.; Gelbrich, T.; Hursthouse, M. B.; Kuhs, W. F.; Shankland, N.; Sowa, H. *CrystEngComm* **2009**, *11*, 1396−1406.

(22) Pogue, J. M.; Marchaim, D.; Kaye, D.; Kaye, K. S. *Pharmacotherapy* **2011**, *31*, 912−21.

(23) Fischbach, M. A. *Curr. Opin. Microbiol.* **2011**, *14*, 519−23.

(24) Al-Omar, M. *Anal. Profiles Drug Subst.* **2004**, *31*, 163−214.

(25) Mazuel, C. *Anal. Profiles Drug Subst.* **1991**, *20*, 557−600.

(26) Turel, I.; Bukovec, P. *Thermochim. Acta* **1996**, *287*, 311−318.

(27) Turel, I.; Bukovec, P.; Quirós, M. *Int. J. Pharm.* **1997**, *152*, 59−65.

(28) Thangadurai, S.; Shukla, S. K.; Srivastava, A. K.; Anjaneyulu, Y. *Acta Pharm.* **2003**, *53*, 295−303.

(29) Wang, P. L.; Feng, Y. L.; Chen, L. A. *Microchem. J.* **1997**, *56*, 229−235.

(30) *SAINT-Plus (including XPREP)*, Version 7.12; Bruker AXS Inc.; Madison, WI, 2004.

(31) Sheldrick, G. M. *Acta Crystallogr.* **2008**, *A64*, 112−122.

(32) Barbour, L. J. *J. Supramol. Chem.* **2003**, *1*, 189−191.

(33) Holzgrabe, U.; Branch, S. K. *Magn. Reson. Chem.* **1994**, *32*, 192−196.

(34) *The Merck Index*, XII ed.; Merck & Co. Inc.: New Jersey, 1996.

(35) Ross, D.; Riley, Ch. *Int. J. Pharm.* **1990**, *63*, 237−250.

(36) Hu, T.; Wang, S.; Chen, T.; Lin, S. *J. Pharm. Sci.* **2002**, *91*, 1351−1357.

(37) Roy, S.; Goud, R.; Babu, N. J.; Iqbal, J.; Kruthiventi, A. K.; Nangia, A. *Cryst. Growth Des.* **2008**, *8*, 4343−4346.

(38) Katdare, A. V.; Ryan, J. A.; Bavitz, J. F.; Erb, D. M.; Guillory, J. K. *Mikrochim Acta Wien III* **1986**, 1−12.

(39) Ravindra, N. V.; Panpalia, G. M.; Sarma Jagarlapudi, R. P. *Acta Crystallgr.* **2009**, *E65*, o303.

(40) Florence, A. J.; Kennedy, A. R.; Shankland, N.; Wright, E.; Al-Rubayi, A. *Acta Crystallogr.* **2000**, *C56*, 1372−1373.

(41) Chongcharoen, W.; Byrn, S. R.; Sutanthavibul, N. *J. Pharm. Sci.* **2008**, *97*, 473−489.

(42) Basavoju, S.; Boström, D.; Velaga, S. P. *Cryst. Growth Des.* **2006**, *6*, 2699−2708.

(43) Mahapatra, S.; Venugopala, K. N.; Guru Row, T. N. *Cryst. Growth Des.* **2010**, *10*, 1866−1870.

(44) Li, X.; Zhi, F.; Hu, Y. *Int. J. Pharm.* **2006**, *328*, 177−182.

(45) Cambridge Structural Database and Cambridge Structural Database system, Version 5.32; Cambridge Crystallographic Data Centre, University Chemical Laboratory: Cambridge England, May 2011.
(46) Fabbiani, F. P. A.; Arlin, J. −B.; Buth, G.; Dittrich, B.; Florence, A. J.; Herbst-Irmer, R.; Sowa, H. *Acta Crystallogr.* **2011**, *C67*, o120−o124.
(47) Sustar, B.; Bukovec, N.; Bukovec, P. *J. Therm. Anal.* **1993**, *40*, 475−481.